Vesicle Array-Templated Large-Area Silica Surface Patterns

Qihui Shi,[†] Jianfang Wang,[†] Michael D. Wyrsta,*,[‡] and Galen D. Stucky*,[†]

*Department of Chemistry and Biochemistry, University of California, Santa Barbara, California 93106, and
Kiowan, Inc., Santa Barbara, California 93103*

Received April 29, 2005; E-mail: stucky@chem.ucsb.edu; mdw@kiowan.com

Micropatterning has applications in a wide range of areas. In contrast to the technological world, where micropatterns are produced lithographically, biological systems provide numerous examples of the formation of biominerals with intricate surface patterns and architectures, which are involved in a variety of biological functions, such as protection and light harvesting.[1]

Biominerals are formed through an intimate association between inorganic and organic materials, where amphiphile-derived vesicles are often involved. Vesicles formed on cell membrane walls provide templates for inorganic material deposition. In addition, vesicle fusion, fission, collapse, and inorganic material deposition often occur synergistically, resulting in the formation of complex patterns over multiple length scales.[2]

Vesicle templating has been used to create materials with complex structures. For example, bowl-shaped depressions have been produced on the surfaces of aluminophosphate spheres using alkylamines as surfactants at 180 °C.[3] Vesicular silica structures have been synthesized using a vesicle-assisted process.[4−6] In contrast to the previous efforts on the vesicle-templated synthesis of spherical particles with intriguing surface features and internal mesostructures, here we report an approach for generating surface patterns of microscale silica features up to areas of 10 mm^2 using vesicle arrays as templates at room temperature. The morphologies of silica features, including convex protrusions, concave depressions, and their hierarchical combinations, are controlled synthetically. It is further demonstrated that these surface patterns can function as arrays of microlenses that are capable of producing numerous images from a common object.

Our vesicle-templating approach makes use of a Pluronic triblock copolymer, L31.[7] The preparation starts with mixing tetraethyl orthosilicate (TEOS), ethanol, and an aqueous HCl solution of pH ∼2. TEOS is prehydrolyzed by stirring at 60 °C for 4 h, and then L31 and dimethylformamide (DMF) are added, giving a molar composition of 1 TEOS:4.0 C$_2$H$_5$OH:4.0 H$_2$O:0.056 L31:0.61 DMF. After the mixture is further stirred vigorously for ∼1 min, an appropriate amount is transferred into an open cylindrical well of 7 mm in diameter and 8 mm in depth. The mixture is gelled and dried in air for 2−4 days, during which a cylindrical transparent monolith forms with surface patterns present on its top surface. The monolith has a diameter of ∼5 mm, and its height varies from 2 to 5 mm, depending on the amount of the solution transferred into the well.

Scanning electron microscopy (SEM) imaging shows that the entire top surfaces of as-prepared monoliths are covered with remarkable patterns of silica features arranged in a roughly hexagonal symmetry (Figure 1a). SEM imaging on tilted monoliths indicates that the silica features are convex protrusions with smooth surfaces (Figure 1b). They are stable under the electron beam of 2−5 keV. Their diameters are relatively uniform, in the range of
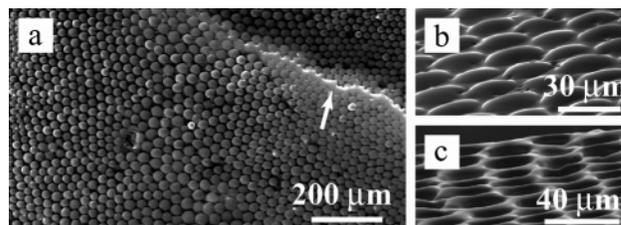
[†] University of California, Santa Barbara.
[‡] Kiowan, Inc.

Figure 1. SEM images of convex silica surface patterns produced on monoliths. (a) A nontilted monolith. The arrow indicates a step on the surface. (b) A tilted monolith. (c) A tilted monolith with its top surface scratched off using a razor blade.
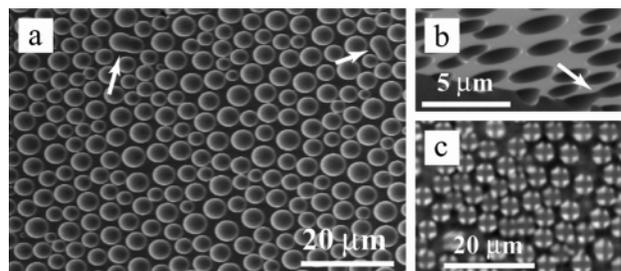

Figure 2. Concave patterns. (a) SEM image of a nontilted monolith. (b) SEM image of a tilted monolith. The arrows in (a) and (b) indicate elongated depressions templated by fused vesicles. (c) Virtual images obtained using a concave surface pattern as a microlens array from a single cross of 20 mm length and 2 mm line width (see Figure S1 in Supporting Information for the explanation of the simultaneous observation of concave depression bottoms and the images of the cross).

10−40 μm. Importantly, SEM imaging on the monoliths with their top surfaces scratched off reveals that each convex protrusion is hollow and approximately hemispherical, with the other half embedded in monoliths (Figure 1c), suggesting that the formation of convex silica protrusions is templated by the vesicles derived from copolymer molecules.

The convex patterns are obtained with TEOS hydrolyzed before being mixed with L31 and DMF. Interestingly, when TEOS is directly mixed with ethanol, HCl solution, L31, and DMF in the same molar ratio without prehydrolysis, large-area patterns of concave silica depressions are produced (Figure 2a,b, and Supporting Information Figures S1a and S1b). The concave depressions are hemispherical with smooth surfaces. Their diameters range from 2 to 6 μm. It is often observed that two concave depressions adhere to each other to form an elongated depression (Figure 2a,b), which we believe is due to vesicle fusion.

The concave surface patterns can be used as microlens arrays to form image arrays from a common object, as demonstrated in Figure 2c, where each concave depression generates a virtual image with a lateral size reduction of ∼6000 from a single cross.[8] They can be further used as masters to generate convex microlens arrays on the surfaces of other materials through replica molding[9] for applications in microlens array reduction photolithography.[10]
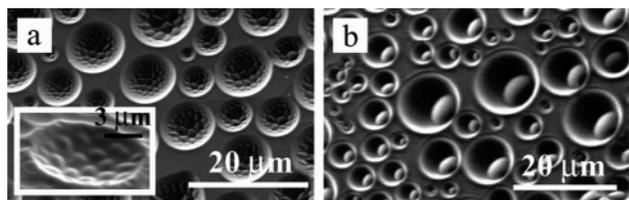
Figure 3. SEM images of hierarchical surface patterns. (a) Each concave depression contains tens of convex protrusions. The inset is an SEM image taken on a tilted monolith. (b) Each concave depression contains one or a few convex protrusions.
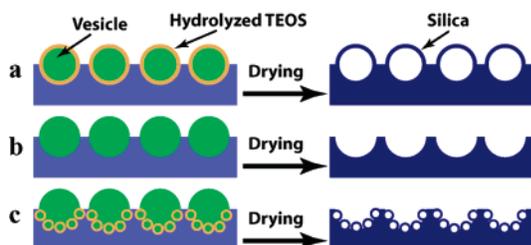

Figure 4. Proposed mechanism of surface patterning. (a) Convex patterns. (b) Concave patterns. (c) Hierarchical patterns.

Compared to concave depressions, convex protrusions only give blurred real images of a common object, which is consistent with the fact that convex protrusions are hollow and spherical.

Surface patterns of hierarchical structures have been further produced when more HCl solution is used and TEOS is not prehydrolyzed. Figure 3 and Figure S2 in Supporting Information show the obtained surface patterns with a molar ratio of 1 TEOS: 4.0 C_2H_5OH:10.0 H_2O:0.056 L31:0.61 DMF. Remarkably, the patterns are composed of larger concave depressions attached with smaller convex protrusions (Figure 3a, inset). Concave depressions have diameters of $1-15$ μm and convex protrusions from 1 to 5 μm. Each concave depression contains from one (Figure 3b) to tens of convex protrusions (Figure 3a). Future efforts are required for the synthetic control of the number of convex protrusions that are contained in each concave depression.

We propose that the formation of surface patterns is templated by L31 vesicle arrays assembled on the surfaces of drying monoliths (Figure 4). The control of the sequence of vesicle formation, TEOS hydrolysis, and silica condensation is crucial not only for pattern replication but also for the generation of convex and concave surface structures. If TEOS is hydrolyzed before being mixed with L31 and DMF, the mixture solution will contain hydrophilic molecular silica species, which can be associated with hydrophilic groups that are exposed on vesicle surfaces through hydrogen bonding. Vesicles will thus be encapsulated with a thin layer of silica species, which are cross-linked to give hollow convex patterns (Figure 4a). If TEOS is directly mixed with L31 and DMF without prehydrolysis, vesicles will form without associated silica species because TEOS is hydrophobic and, thus, leave imprints on the surfaces of drying monoliths, producing concave patterns (Figure 4b). Furthermore, an increase in the amount of water without TEOS prehydrolysis will lead to the formation of a hierarchy of vesicles. Vesicles formed in the beginning will not be encapsulated with silica species, while those formed after TEOS hydrolysis will carry silica species on their surfaces. The vesicles encapsulated with silica species will adhere and pack around the vesicles formed in the beginning, resulting in the generation of hierarchical patterns of larger concave depressions attached with smaller convex protrusions (Figure 4c).

Both L31 and DMF are important in the formation of surface patterns. We have tried other copolymers, including L64, L121, P65, P85, P103, P123, F68, F88, and F127,[11] and other solvents,

including octane, tetrahydrofuran, acetone, and hexane. It is found that only the use of L31 together with DMF leads to the production of patterns under our experimental conditions. Up to date, there have been only a few reports on the formation of vesicles from Pluronic copolymers.[6,12] In our experiments, L31 is readily dissolved in ethanol. As ethanol evaporates, the solubility of the hydrophobic block gradually decreases, driving the assembly of L31. Because of the short hydrophilic blocks relative to the hydrophobic blocks, and therefore a small headgroup area, L31 copolymers pack into a lamellar phase. DMF in the solution not only functions as a cosolvent but also interacts with the headgroup of L31 through hydrogen bonding. This interaction serves to enlarge the headgroup area of L31, which consequently causes curvature and transforms lamellar layers into vesicles. It is noted that similar methods have been used before to prepare mesostructured silica monoliths, where F127 and P123 were used as a surfactant, water and ethanol as solvents, but only interior mesostructures were investigated.[13]

In summary, we have demonstrated vesicle array-templated surface patterning of microscale silica features, including convex protrusions, concave depressions, and their combinations, which can be synthetically controlled. We believe that our approach is of implications for chemically designing and tailoring hierarchically structured materials with desired functions.

Supporting Information Available: Large-area SEM images of surface patterns and schematics showing the optical system for recording image arrays and the image formation. This material is available free of charge via the Internet at http://pubs.acs.org.

References

(1) Aizenberg, J.; Tkachenko, A.; Weiner, S.; Addadi, L.; Hendler, G. *Nature* **2001**, *412*, 819–822.
(2) (a) Mann, S.; Ozin, G. A. *Nature* **1996**, *382*, 313–318. (b) Sanchez, C.; Arribart, H.; Guille, M. M. G. *Nat. Mater.* **2005**, *4*, 277–288.
(3) (a) Oliver, S.; Kuperman, A.; Coombs, N.; Lough, A.; Ozin, G. A. *Nature* **1995**, *378*, 47–50. (b) Oliver, S.; Coombs, N.; Ozin, G. A. *Adv. Mater.* **1995**, *7*, 931–935.
(4) (a) Tanev, P. T.; Pinnavaia, T. J. *Science* **1996**, *271*, 1267–1269. (b) Tanev, P. T.; Liang, Y.; Pinnavaia, T. J. *J. Am. Chem. Soc.* **1997**, *119*, 8616–8624. (c) Kim, S. S.; Zhang, W. Z.; Pinnavaia, T. J. *Science* **1998**, *282*, 1302–1305.
(5) (a) Hubert, D. H. W.; Jung, M.; Frederik, P. M.; Bomans, P. H. H.; Meuldijk, J.; German, A. L. *Adv. Mater.* **2000**, *12*, 1286–1290. (b) Rana, R. K.; Mastai, Y.; Gedanken, A. *Adv. Mater.* **2002**, *14*, 1414–1418.
(6) Sun, Q. Y.; Kooyman, P. J.; Grossmann, J. G.; Bomans, P. H. H.; Frederik, P. M.; Magusin, P. C. M. M.; Beelen, T. P. M.; van Santen, R. A.; Sommerdijk, N. A. J. M. *Adv. Mater.* **2003**, *15*, 1097–1100.
(7) Pluronic copolymers are poly(ethylene glycol)−*block*−poly(propylene glycol)−*block*−poly(ethylene glycol), and L31 is $EO_2PO_{16}EO_2$.
(8) See Figures S1c and S1d in Supporting Information for the schematic illustrations of the optical system for recording image arrays and the image formation from a single concave depression, respectively.
(9) Xia, Y. N.; Whitesides, G. M. *Angew. Chem., Int. Ed.* **1998**, *37*, 550–575.
(10) (a) Wu, M.-H.; Whitesides, G. M. *Adv. Mater.* **2002**, *14*, 1502–1506. (b) Wu, H. K.; Odom, T. W.; Whitesides, G. M. *J. Am. Chem. Soc.* **2002**, *124*, 7288–7289.
(11) L64, $EO_{13}PO_{30}EO_{13}$; L121, $EO_5PO_{70}EO_5$; P65, $EO_{20}PO_{30}EO_{20}$; P85, EO_{26}-$PO_{39}EO_{26}$; P103, $EO_{17}PO_{56}EO_{17}$; P123, $EO_{20}PO_{70}EO_{20}$; F68, $EO_{80}PO_{30}$-EO_{80}; F88, $EO_{100}PO_{39}EO_{100}$; F127, $EO_{106}PO_{70}EO_{106}$.
(12) (a) Schillén, K.; Bryskhe, K.; Mel'nikova, Y. S. *Macromolecules* **1999**, *32*, 6885–6888. (b) Bryskhe, K.; Jansson, J.; Topgaard, D.; Schillén, K.; Olsson, U. *J. Phys. Chem. B* **2004**, *108*, 9710–9719.
(13) (a) Melosh, N. A.; Lipic, P.; Bates, F. S.; Wudl, F.; Stucky, G. D.; Fredrickson, G. H.; Chmelka, B. F. *Macromolecules* **1999**, *32*, 4332–4342. (b) Melosh, N. A.; Davidson, P.; Chmelka, B. F. *J. Am. Chem. Soc.* **2000**, *122*, 823–829. (c) Yang, H. F.; Shi, Q. H.; Tian, B. Z.; Xie, S. H.; Zhang, F. Q.; Yan, Y.; Tu, B.; Zhao, D. Y. *Chem. Mater.* **2003**, *15*, 536–541.

JA052815J